

1                   **Absolute abundance estimates from shallow water baited underwater camera surveys; a**  
2                   **stochastic modelling approach tested against field data**

3  
4                   K.M. Dunlop <sup>a,\*</sup>, G.D. Ruxton <sup>b</sup>, E.M. Scott <sup>c</sup>, D.M. Bailey <sup>a</sup>

5  
6 <sup>a</sup> Institute of Biodiversity, Animal Health and Comparative Medicine, University of Glasgow, Glasgow,  
7 G12 8QQ, UK

8 <sup>b</sup> School of Biology, University of St Andrews, St Andrews, Fife, KY16 9TH, UK

9 <sup>c</sup> School of Mathematics and Statistics, University of Glasgow, Glasgow, G12 8QQ, UK

10  
11 \* Corresponding author current address. Monterey Bay Aquarium Research Institute, 7700 Sandholdt Road,  
12 Moss Landing, CA 95039, USA, Tel.: +1 831 775 1773; fax: +1 831 775 1638.

13 *E-mail address:* [kdunlop@mbari.org](mailto:kdunlop@mbari.org) (K.M. Dunlop).

14  
15 **Abstract**

16  
17 Baited underwater cameras are becoming a popular tool to monitor fish and invertebrate populations within  
18 protected and inshore environments where trawl surveys are unsuitable. Modelling the arrival times of  
19 deep-sea grenadiers using an inverse square relationship has enabled abundance estimates, comparable to  
20 those from bottom trawl surveys, to be gathered from deep-sea baited camera surveys. Baited underwater  
21 camera systems in the shallow water environments are however, currently limited to relative comparisons of  
22 assemblages based on simple metrics such as Max<sub>N</sub> (maximum number of fish seen at any one time). This  
23 study describes a stochastic simulation approach used to model the behaviour of fish and invertebrates  
24 around a BUC system to enable absolute abundance estimates to be generated from arrival patterns.  
25 Species-specific models were developed for the tropical reef fishes the black tip grouper (*Epinephelus*  
26 *fasciatus*) and moray eel (*Gymnothorax* spp.) and the Antarctic scavengers; the asteroid (*Odontaster*  
27 *validus*) and the nemertean worm (*Parbolasia corrugatus*). A sensitivity analysis explored the impact of  
28 input parameters on the arrival patterns (Max<sub>N</sub>, time to the arrival of the first individual and the time to  
29 reach Max<sub>N</sub>) for each species generated by the model. Sensitivity analysis showed a particularly strong link  
30 between Max<sub>N</sub> and abundance indicating that this model could be used to generate absolute abundances  
31 from existing or future Max<sub>N</sub> data. It in effect allows the slope of the Max<sub>N</sub> vs. abundance relationship to be  
32 estimated. Arrival patterns generated by each model were used to estimate population density for the focal  
33 species and these estimates were compared to data from underwater visual census transects. Using a Bland-  
34 Altman analysis, baited underwater camera data processed using this model were shown to generate  
35 absolute abundance estimates that were comparable to underwater visual census data.

36  
37 **Highlights:**

- 38 - Modelling the behaviour of fish and invertebrates around a baited camera system  
39 - Models developed for tropical fish and Antarctic invertebrates  
40 - Abundance estimates calculated and compared to data from visual census transects

41 - Comparable abundance estimates generated by the model and transects

42 **Keywords:** baited underwater cameras; modeling; fish and invertebrate surveys; underwater visual census

43

44 **Abbreviations:**

45 BUC: Baited underwater camera

46  $Max_N$ : Maximum number of individuals, of the same species, appearing on the field of view in any one  
47 frame over the whole deployment

48  $T_{arrival}$ : Time to the arrival of the first individual from each species

49  $T_{maxN}$ : Time to the maximum number of individuals observed at one time

50 UVC: Underwater visual census

51

## 52 **1. Introduction**

53

54 Abundance estimates of marine populations, that are both accurate, close to the true abundance, and  
55 precise, repeatable under the same conditions, are important to understand changes in marine populations or  
56 communities (Farnsworth et al., 2007) and to help achieve sustainable management and effective  
57 conservation objectives (Collins et al., 2002). For marine fish and invertebrate populations the majority of  
58 this data has been collected using trawl surveys (Fitzpatrick et al., 2012; Johnson et al., 2012), which are  
59 difficult in abyssal environments and unsuitable in marine protected areas (Bailey et al., 2007). Baited  
60 underwater camera (BUC) systems have therefore been used in many studies to gather data on deep-sea  
61 scavenging fauna (Farnsworth et al., 2007) and fish assemblages in protected areas (Willis and Babcock,  
62 2000; McLean et al., 2010). However, to use BUC data to produce absolute abundance estimates of fish  
63 and invertebrate populations requires a detailed understanding of the physical and biological parameters  
64 involved in the process of animals detecting and following the bait plume to the camera (Priede et al., 1994;  
65 Bailey et al., 2007).

66

67 Bait plume dispersal from a point source, its detection by fish or invertebrates and their arrival at the  
68 source, is influenced by a number of environmental and biological factors (Collins et al., 2002; Stoner,  
69 2004). The odour from the bait disperses as a plume into the surrounding water on currents (Reidenbach  
70 and Koehl, 2011). The velocity and direction of currents will affect the length and lateral dispersal of the  
71 plume as well as its dispersal direction (Bailey and Priede, 2002; Dorman et al., 2012). The dispersal of  
72 odour plumes is also affected by turbulence within the aquatic environment (Meager and Batty, 2007), the  
73 topography over which it travels (Collins et al., 1999; Collins et al., 2002; Reidenbach and Koehl, 2011) and  
74 the characteristics and persistence of the bait (Bailey and Priede, 2002; Stoner, 2004). Fish and  
75 invertebrates have evolved olfactory organs with chemosensory abilities that allow them to detect odour  
76 plumes and follow them to their source (Reidenbach and Koehl, 2011). The area within the odour plume  
77 where the odour concentration is above the threshold which organisms can detect is known as the 'active  
78 space' (Sigler, 2000; Stoner, 2004). The probability of the fish entering the active space of the bait plume  
79 will be dependent on their search behaviours (Dorman et al., 2012), including their swimming speed and  
80 position in the water when foraging (Stoner, 2004), as well as the abundance and distribution of the

81 population (Armstrong et al., 1992). Once the plume has been detected, the fish will decide whether to  
82 follow it based on the feeding motivation that the bait provides (Dorman et al., 2012). The time that  
83 individuals remain at the bait will be determined by the availability of food within the environment  
84 (Charnov, 1976) as well as the competition and interactions with other scavengers at the bait (Armstrong et  
85 al., 1992; Bailey and Priede, 2002; Dunlop et al., 2014).

86

87 The process of bait plume detection, attraction and arrival of the deep sea grenadier *Coryphaenoides*  
88 *armatus* at a BUC was modelled using an inverse square relationship:

89

$$90 \quad n = c/t_{\text{arr}}^2$$

91

92 where  $n$  is the number of fish per square kilometre and  $c$  is a constant, dependent upon the current velocity  
93 and through water swimming speed of the fish towards the BUC system (Priede et al., 1990; Priede and  
94 Bagley, 2000).  $t_{\text{arr}}$  represents the time elapsed between the beginning of the camera deployment and the  
95 arrival of the first fish. The model was developed by Priede et al., (1990) to allow scavenger density to be  
96 estimated from their arrival rates at the BUC in conjunction with information on the odour plume spreading  
97 characteristics, current velocities and fish swimming speed. The staying time of deep-sea grenadiers at the  
98 BUC can be estimated using the relationship:

99

$$N_{\beta} = \frac{\alpha_0}{x}(1 - e^{-\beta x})$$

100

101 where  $N_{\beta}$  is the maximum number of fish present after a certain period of time,  $\alpha_0$  the initial rate of fish  
102 arrival at time zero,  $e$  the exponential constant and  $x$  a constant representing the decay of the odour plume  
103 from dilution and bait consumption (Priede et al., 1990). Arrival rates are of interest as a bait placed  
104 amongst an abundant scavenger population has a greater chance of being reached by an individual quickly  
105 (Bassett and Montgomery, 2011). The arrival times of deep-sea grenadiers at a BUC in two sites in the  
106 North Atlantic were modelled in the above manner to produce estimates of abundance which were  
107 comparable to those from bottom trawl surveys from approximately the same area and time (Armstrong et  
108 al., 1992; Priede and Merrett, 1996). However, when applied to fish arrival times on the Mid-Atlantic Ridge  
109 there was no correlation between BUC generated abundances and those estimated from trawls (Bailey et al.,  
110 2007).

111

112 The use of BUC systems in shallow waters have enabled relative comparisons of both fish and  
113 invertebrate assemblages in the tropical (McLean et al., 2010; Moore et al., 2010), temperate (Willis et al.,  
114 2003) and the Antarctic environments (Smale et al., 2007) between areas of different protection status  
115 (Willis and Babcock, 2000; Westera et al., 2003), habitat type (Moore et al., 2010) and disturbance pressure  
116 (Smale et al., 2007). The majority of studies have used the maximum number of individuals, of the same  
117 species, appearing in the field of view in any one frame over the whole deployment ( $\text{Max}_N$ ) as an index of  
118 relative abundance (Willis and Babcock, 2000; Stoner et al., 2008).  $\text{Max}_N$  avoids the repeated recording of  
119 individuals that leave and re-enter the camera field of view and usually less than the count of all animals

120 visiting the bait (McLean et al., 2010; Harvey et al., 2012). Some surveys have also used the time to the  
121 arrival of the first individual from each species ( $t_{\text{arrival}}$ ) and time to the maximum number of individuals  
122 observed at one time ( $t_{\text{maxN}}$ ) (Willis and Babcock, 2000; Jones et al., 2003). In the shallow water  
123 environment however, the development of models of the process of fish or invertebrate arrival at BUCs has  
124 been limited (Stoner et al., 2008; Langlois et al., 2012). Heagney et al., (2007) investigated whether abyssal  
125 scavenger arrival models could be applied to shallow mid-water baited underwater video data. Existing  
126 models appropriate for deep-sea BUC studies with long soak times and where scavengers approached more  
127 slowly, were found unsuitable for shallow water BUC studies with much shorter soak times and which  
128 attract many fast moving species (Heagney et al., 2007). Rapid arrival patterns of shallow water fish result  
129 in overestimated abundance due to the inverse square law of the abyssal model (King et al., 2006; Stobart et  
130 al., 2007). Compared to the shallow water environment, currents in the abyss are relatively constant, so an  
131 assumption of a constant current speed and direction is more suitable (Heagney et al., 2007; King et al.,  
132 2008). The assumptions of deep-sea models also cannot be applied to describe the foraging behaviours of  
133 shallow water fish species, which also use sight, as well as chemoreception, to find food (Ellis and  
134 DeMartini, 1995; Stobart et al., 2007). The time related metrics used in the deep-sea such as,  $t_{\text{arrival}}$  and  $t_{\text{maxN}}$ ,  
135 have not correlated well with other surveys methods in some shallow water BUC surveys (Stoner et al.,  
136 2008; Willis and Babcock, 2000).

137

138 The area sampled by the active space of the odour plume is largely unknown in shallow BUC surveys.  
139 Concerns have been raised regarding the effect of localised environmental conditions, such as topography  
140 and current conditions, on plume dynamics making it difficult to make comparisons between areas (Taylor  
141 et al., 2013; Watson et al., 2009). Surveys assume that a comparable area is sampled by each deployment,  
142 however, this will often be untrue if current conditions vary (Heagney et al., 2007). The importance of the  
143 currents on the dynamics of bait plume dispersal and subsequent fish arrival patterns have been highlighted  
144 in several studies in the mid water (Heagney et al., 2007) and demersal environments (Dorman et al., 2012).  
145 The unknown sample area of shallow water BUC surveys also makes it difficult to make comparisons with  
146 abundance estimates from other survey methods. Several studies have investigated the differences in fish  
147 and invertebrate studies recorded by BUC and UVC surveys (Langlois, 2006; Watson et al., 2010),  
148 however, conclusions regarding comparisons have been difficult as the area sampled cannot be directly  
149 compared (Langlois et al., 2010).

150

151 A model to determine the absolute measures of shallow water fish or invertebrate abundance from  
152 arrival patterns at a BUC would involve developing an area based bait dispersion model using in-situ  
153 measurements of current speed and direction (Heagney et al., 2007). The mechanistic models outlined by  
154 Priede et al., (1990) to estimate the abundance of deep-sea demersal fish from first arrival times are  
155 deterministic. However, the arrival rate of fish is stochastically related to population abundance and the  
156 factors governing aspects of shallow water fish movement are often assumed to be well represented by  
157 random distribution (Farnsworth et al., 2007). This means it is important to include stochastic elements to  
158 mechanistic models. The physical factors, current distribution and velocity, observed around the camera  
159 system also have a random distribution within a particular range. Therefore it is important to introduce this

160 random aspect into models to describe fish attraction and arrival at a BUC system. Stochastic models that  
 161 incorporate both the predictable and random aspects of a process, are increasingly being used to build our  
 162 understanding of complex natural ecosystems (Brown and Kulasiri, 1996). Farnsworth et al., (2007) also  
 163 modelled the arrival process of deep-sea demersal scavengers at the BUC using the addition of stochastic  
 164 elements to deterministic models. Farnsworth's (2007) models unfortunately did not include a mechanism  
 165 to reverse the process and calculate abundances from arrival patterns. The models also required a very large  
 166 number of assumptions and parameters, making them difficult to implement for many BUC users.

167

168 The primary objective of the present study was to develop a stochastic modelling approach to enable the  
 169 estimation of the absolute abundance of fish and invertebrates using arrival data collected using a shallow  
 170 water BUC system. This involved the development of species-specific models for two fish and two  
 171 invertebrate species observed in tropical and Antarctic BUC surveys. A global sensitivity analysis was used  
 172 to determine the impact of model parameters on the arrival pattern produced by the model. A secondary  
 173 objective, following the development of an effective modelling methodology, was to demonstrate how  
 174 absolute abundance estimates can be generated from BUC data using the methodology. The achievement of  
 175 this objective was assessed by comparing the model absolute abundance outputs to those from  
 176 corresponding underwater visual census (UVC) transects. It was hypothesised that 1), the sensitivity  
 177 analysis would show which model variables have an effect upon the arrival pattern of fish or invertebrates at  
 178 the BUC and what aspects of the arrival pattern variable are affected the most (i.e.  $\text{Max}_N$ ,  $t_{\text{arrival}}$  and  $t_{\text{maxN}}$ )  
 179 and 2), that the modelling methodology would generate absolute abundance estimate that were comparable  
 180 to those from corresponding UVC surveys.

181

## 182 2. Materials and Methods

183

### 184 2.1. Model outline

185

186 The simulation was built in MATLAB (R2010b) using the movement of an individual fish around a  
 187 BUC system within a designated area. A bait plume was plotted and the area covered ( $B_a$ ,  $\text{m}^2$ ) was  
 188 described as a sector of a circle, using the three equations below. The length of the plume ( $L_{pl}$ , m) was  
 189 calculated using a radius described as the mean current speed ( $V_w$ ,  $\text{ms}^{-1}$ ) recorded throughout the  
 190 deployment multiplied by the simulation time ( $T$ , seconds). The plume therefore expanded with every time  
 191 step of the simulation. The plume angle ( $Pl_{\theta}$ , radians) was calculated from the inverse tangent of the  
 192 diffusional velocity ( $B_y$ ,  $\text{ms}^{-1}$ ), divided by the current speed ( $V_w$ ,  $\text{ms}^{-1}$ ). The relationship between these  
 193 model parameters is described in the equations:

$$L_{pl} = V_w T$$

$$Pl_{\theta} = 2 \tan^{-1} \left( \frac{B_y}{V_w} \right)$$

$$B_a = \left( \frac{\theta}{2} \right) L_{pl}^2$$

194 Simulations depict the movement of a population of a fixed abundance within a defined area ( $A$ ,  $\text{m}^2$ ). Prior  
 195 to detection of the bait plume fish move at a cruising speed ( $V_{cr}$ ,  $\text{ms}^{-1}$ ) or are stationary, and turned a random

196 number of times ( $T_r$ ) within a set time period known as the turning interval ( $Int_{tr}$ , seconds). The direction  
 197 within which the fish travels after each turn ( $D_r$ , radians) was randomly selected (independently for each  
 198 individual).

199

200

$$D_r = rand(0, 360)$$

$$Int_{tr} = rand(0, T_r) * T_r$$

201

202 The starting point ( $P_{st}(x, y)$ ) was selected (again independently for each individual) from a random  
 203 position within the simulation area ( $A, m^2$ ) using the formula below:

204

$$(P_{st}(x, y)) = rand\left(-\frac{A}{2}, \frac{A}{2}\right)$$

205

206 The distance travelled per time step ( $D_s$ , m) was calculated by dividing the cruising speed by the time  
 207 resolution ( $T_r$ , seconds). Distance travelled in the x and y axis ( $D_s(x, y)$ ) was found by multiplying the  
 208 cruise speed divided by the simulation time resolution (length of the time-step used in simulations) and  
 209 multiplying this by sine and cosine of the direction ( $D_r$ , radians):

210

211

$$D_s(x) = \frac{V_{cr}}{T_r} \sin(D_r)$$

212

$$D_s(y) = \frac{V_{cr}}{T_r} \cos(D_r)$$

213

214 The distance to the camera ( $D_{cm}(x, y)$ ) was calculated by taking the square root of the distance travelled in  
 215 the x and y axis:

$$D_{cm}(x, y) = \sqrt{D_s(x, y)^2}$$

216

217 When the distance to the camera ( $D_{cm}(x, y)$ ) is less than the radius associated with the circular bait area  
 218 ( $B_a, m^2$ ) the fish is considered to have encountered the bait plume area. On encounter the fish turns into an  
 219 approach angle  $app(\theta)$  calculated using:

220

$$app(\theta) = (180, 360, 0, -180 \tan^{-1} D_s\left(\frac{x}{y}\right))$$

221

222 (the angle used in this equation depends upon the position on the fish when the bait plume is encountered).

223 This change in direction causes the fish to swim directly upstream towards the bait at a through-water

224 approach speed up the plume towards the camera ( $V_{f_{sa}}, ms^{-1}$ ). This speed is faster than the cruising

225 swimming speed and was calculated from observation of fish max swimming speed in previous published

226 studies. Current speed ( $V_w, ms^{-1}$ ) is subtracted to account for the fish swimming upstream against the

227 current. Once in the bait plume the distance travelled towards the camera and its relation to the camera

228 position is recalculated using the through-water approach speed ( $V_{f_{sa}}, ms^{-1}$ ):

229

230

$$D_s(x) = \frac{V_{f_{sa}}}{T_r} \sin(D_r)$$

231

$$D_s(y) = \frac{V_{f_{sa}}}{T_r} \cos(D_r)$$

232

233 Upon reaching the bait the individual will remain there for a “staying time” ( $S_t$ , seconds) found by taking a  
234 random time between a pre-determined interval. This was multiplied by the time resolution ( $T_r$ , seconds) of  
235 the simulation:

$$S_t = rand([1800, T_r])$$

236

237 After remaining at the camera for the staying time the fish is removed from the simulation as it is assumed  
238 to have reached satiation or decided to forage elsewhere. Simulations run for 60 or 90 minutes and record  
239 the total number of fish, or invertebrates, present at the bait every 30 seconds, the same interval is used in  
240 the in-situ BUC studies. For the invertebrates studied here staying time was set till the simulation end. The  
241 model is depicted in as a diagram in Fig. 1.

242

## 243 2.2. General assumptions

244

245 Fish or invertebrates are assumed to act independently of each other at all stages of the simulation and to  
246 always react to the bait plume on encounter. The bait plume was always spread from the origin of the  
247 coordinate system used in the simulations and assumed to disperse in a single direction. The present model  
248 assumes a constant plume concentration and represents a framework that can be combined with fluid  
249 dynamics models of bait plume dispersal from a point source in the future to enable the dilution of the  
250 plume concentration and changes in current direction to be incorporated into the models.

251

252 Simulations were developed for four species; the grouper *Epinephelus fasciatus* and moray eels of the  
253 genus *Gymnothorax* spp. recorded in the tropical Gulf of Aqaba and the Antarctic scavenging invertebrates  
254 *Odontaster validus* and *Parbolasia corrugatus*. The BUC system consisted of a digital stills camera  
255 (SeaLife DC800 or DC1000) enclosed in an underwater housing. No additional light was required for work  
256 in the Gulf of Aqaba, but in Antarctica the camera was synchronized, via optical cables, with two variable-  
257 power digital slave strobe light units (Epoque ES-23DS). The camera was placed in time lapse mode (30 s  
258 intervals). The camera equipment was supported on an L-shaped frame of aluminium tubing. A u-shaped  
259 bracket holding the camera was bolted to the vertical element of the frame and angled downwards at 60° to  
260 view the mesh bait bag attached to the far end of a horizontal pole. 200 g of either chopped fish (*Sparus*  
261 *aurata* and *Dicentrarchus labrax*) in the Gulf of Aqaba or chopped Antarctic invertebrates (*Ophionotus*  
262 *victoriae*, *O. validus*, *Sterechinus neumayeri* and *Laternula elliptica*) were used as bait. The system was  
263 deployed from a boat and lowered to the seabed or placed by a SCUBA diver. A ballast weight (c10kg) held  
264 the camera system to the seabed and it was held upright in the water column by two small mid-water buoys.  
265 At the end of deployments the camera system was recovered either by hauling on a recovery line or by  
266 attachment and inflation of a lifting bag by SCUBA divers.

267 Data on swimming or crawling speeds, the turning frequency and aspects of the foraging behaviours for  
268 each species were determined from published studies (Fulton, 2007; D'Aout and Aerts, 1999; Clarke and  
269 Prothero-Thomas, 1997; Kidawa, 2001; Bshary et al., 2006) (Table 1). Estimations of staying time were  
270 based on observation of individuals in BUC deployments. For the tropical species it was difficult to identify  
271 individuals to calculate their staying time at the bait and estimations were taken from observation of the  
272 number of consecutive images an individual of that species was observed in. Current velocity was recorded  
273 during Antarctic deployments using a Nortek Aquadopp Acoustic Doppler current meter (Aquadopp  
274 Current Meter, Nortek, USA) while for the Gulf of Aqaba data an Acoustic Doppler Current Profiler  
275 between 10 m and 1 km from BUC deployments was used. Current meter measurements provided the  
276 current ranges within which the simulation could operate.

277 All BUC deployments had a matching underwater visual census (UVC) transect at the same location and  
278 depth making up on station. In the Gulf of Aqaba an area of 100 m<sup>2</sup> was swum once (50 x 2 m transect) and  
279 the numbers of *E. fasciatus* and *Gymnothorax* spp. were recorded on a slate (32 stations total, eight at each  
280 at 5, 10, 15 and 20 m). In Antarctica the density of *O. validus* and *P. corrugatus* was recorded from  
281 analysis of images from a 25 x 0.5 m UVC transect of continuous stills images (18 stations total, six each at  
282 5, 10 and 25 m).

283

284 The ranges of input parameters for each model are described in Table 1. The current speeds observed  
285 during the BUC deployments in both the Antarctic and the Gulf of Aqaba were approximately comparable  
286 to the current speeds measured in the deep-sea environment by Sainte-Marie and Hargrave, (1987).  
287 Therefore, due to the lack of measurements of the diffusional velocities the same velocity, 10<sup>-3</sup> m s<sup>-1</sup>, used to  
288 model the arrival of scavengers at a baited camera by Sainte-Marie and Hargrave, (1987) was used.

289

290 Moray eels of the genus *Gymnothorax* and blacktip groupers (*E. fasciatus*) are ambush predators highly  
291 associated with rocky reefs and crevices and will defend a small territory (Gibran, 2007). Therefore in  
292 simulations of *Gymnothorax* spp. and *E. fasciatus* movement around the BUC system individuals were  
293 relatively slow moving prior to the detection of the bait plume. Antarctic invertebrate scavengers are slow  
294 moving compared to the tropical fish therefore BUC deployments in the shallow water Antarctic  
295 environment lasted for 1.5 h. The invertebrates also crawl along the seabed so current velocity was not  
296 subtracted from the approach velocity. Both Antarctic scavengers remained stationary prior to the detection  
297 of an odour plume and on reaching the bait scavengers remained there till the end of the simulation as  
298 observed in BUC deployments.

299

### 300 2.3. Data analysis

301

302 Models generated an arrival patterns for fish or invertebrates at the bait based on a predicted number  
303 present every 30 s, to produce a dataset in the same form as that from in-situ BUC deployments. Max<sub>N</sub>,  
304 t<sub>arrival</sub> and t<sub>maxN</sub> were used to describe the arrival pattern of fish or invertebrates at the BUC. This sensitivity  
305 analysis enabled the dependence of the fish or invertebrate arrival pattern output by the model on input  
306 parameters to be determined and was used to test hypothesis one. A global sensitivity analysis was



307 performed on each species-specific model to determine the impact of the input parameters; population  
308 abundance, current speed, diffusional velocity, swimming speed before contact with the odour plume,  
309 approach speed and staying time (Table. 1). Each input parameter was set to be randomly selected from the  
310 full range of potential values and each of the four models was run 300 times to ensure that the full range of  
311 potential input parameters was considered. This was checked by plotting a histogram of the distribution of  
312 the input parameters and was also used to ensure that the range of input values had a random distribution.  
313 Both the marginal and bivariate simulated factor distributions were explored to ensure that coverage of the  
314 factor space was extensive (Saltelli, 2000).

315

316 A stepwise regression was performed in R (version 3.0.2, The R Development Core Team, 2013) to  
317 examine the relationship between the input parameters and the model output abundance indices;  $Max_N$ ,  
318  $t_{arrival}$  and  $t_{maxN}$ . The relationship between any input parameter identified as having a significant effect on  
319  $Max_N$ ,  $t_{arrival}$  and  $t_{maxN}$  was plotted in a scatter plot. The relationship between the model parameters and the  
320 BUC abundance indices were unknown as this early stage of model development and the stepwise  
321 regression was used as a tool to explore these relationships. The analysis of the influence of model input  
322 parameters on the resultant fish or invertebrate arrival pattern highlighted which parameters were important  
323 to calibrate with in-situ measurements.

324

#### 325 *2.4. Producing absolute abundance estimates from BUC data*

326

327 Any parameters with a significant effect were parameterised using an in-situ measurement of this  
328 variable where available. For example, if current speed had a significant impact on the  $Max_N$  then the  
329 current speed from the in-situ BUC deployment providing the camera data was used to produce an  
330 abundance estimate was used as a model input. Those identified as having no significant impact on the  
331 model output were set to be selected randomly from a range of suitable values for that measure. However,  
332 for some parameters an in-situ measurement was not available and values within the models had to remain  
333 as the estimates ranges. These parameters were highlighted as those requiring future measurement to  
334 improve the accuracy of the model outputs.

335

336 To produce absolute abundance estimates using the modelling methodology a suitable range of estimated  
337 population abundances must be first input into the model. In practice these estimates could be derived from  
338 previous surveys using other methods, literature for similar areas or be best guesses. In the case of this  
339 validation exercise corresponding UVC surveys from the same position and approximately the same time as  
340 the BUC deployments were used to find a suitable abundance range for the tropical and Antarctic models.  
341 Each single population abundance input into the model produced a BUC arrival pattern. For example, if an  
342 abundance range of 1 - 100 individuals was used 99 arrival patterns would be produced. The arrival  
343 patterns produced by the model were compared to the arrival patterns produced by the corresponding BUC  
344 survey. The R-squared value of the slope fitted to the arrival curve of individuals at the camera with time  
345 was used to find a match between model and BUC arrival patterns. Once a match was found the population  
346 abundance input into the model to produce that arrival pattern is recorded as the model's best estimate of the

347 absolute abundance of the fish or invertebrate population surveyed by the BUC system. This process is  
348 illustrated in Fig. 2 where the arrival pattern from five model runs of the model of *E. fasciatus* movement  
349 around the BUC can be compared to that of the in-situ BUC arrival pattern.

350

351 The absolute abundance estimate produced using the model methodology and field BUC data were  
352 compared to those generated by corresponding UVC surveys to validate the ability of the model to produce  
353 accurate abundance estimates. Models describing the movement of the two tropical fish species and the two  
354 Antarctic invertebrate scavengers in relation to the BUC system were validated using transect data. BUC  
355 absolute abundance estimates were compared to those from the corresponding UVC surveys using a Bland-  
356 Altman analysis (Bland and Altman, 1986). A Bland-Altman analysis is used to compare two methods of  
357 measurement, usually a new method with an established one (Bland and Altman, 1986). In this study the  
358 UVC represents the established method for measuring fish and invertebrate absolute abundance and the  
359 BUC the new method. The Bland-Altman plots show the mean difference between the two corresponding  
360 measurements from both methods, known as ‘the bias’, and the 95% limits of agreement as +/- 1.95 SD of  
361 the mean difference. The plot enables visual judgement of the agreement between the measurements and  
362 the smaller the range between the measurements the better the match (Bland and Altman, 1986; Bland and  
363 Altman, 1995). An analysis showing no significant systematic bias between the two methods would show  
364 the majority of the data points within the confidence limits and that points would have a symmetrical around  
365 zero. A Bland and Altman analysis was performed in the R package ‘MethComp’ and a Bland-Altman plot  
366 and measures of the test bias test were produced to compare the measurements of absolute abundance using  
367 the UVC and tropical and Antarctic BUC models (Fig. 3).

368

### 369 3. Results

370

#### 371 3.1. Sensitivity analysis

372

373 The input parameters (abundance, current speed, approach speed, cruising speed, diffusional velocity  
374 and staying time) produced by 300 runs of the 4 models were plotted in frequency histograms and their  
375 distribution was random and encompassed the full range of potential input parameters. Sensitivity analysis  
376 revealed that the model input parameters explained a large proportion of the variability in the Max<sub>N</sub> output  
377 of the 4 models. Input parameters explained less of the variability in the time-based metrics ( $t_{\text{arrival}}$  and  
378  $t_{\text{maxN}}$ ). Abundance was the model input parameter that had the greatest impact on the Max<sub>N</sub>,  $t_{\text{arrival}}$  and  $t_{\text{maxN}}$   
379 outputs from the model for all 4 species.

380

381 For both tropical models the parameter population abundance explained a large proportion of the  
382 variability in the Max<sub>N</sub> output; *E. fasciatus* ( $y = 0.73x + 0.71$ ; R-sq (adj) = 91.74;  $P < 0.0001$ ) and for  
383 *Gymnothorax* spp. ( $y = 0.57x + 0.49$ ; R-sq (adj) = 97.99;  $P < 0.0001$ ). Input parameters explained less of  
384 the variability in the  $t_{\text{arrival}}$  of tropical fish at the bait. Population abundance had a small but significant  
385 effect on *E. fasciatus* ( $y = 61.81x + 217.89$ ; R-sq (adj) = 18.16;  $P < 0.0001$ ) and *Gymnothorax* spp.  $t_{\text{arrival}}$  ( $y$   
386 =  $-54.21x + 83.89$ ; R-sq (adj) = 30.17;  $P < 0.0001$ ). Current speed also had a significant impact on

387 *Gymnothorax. spp.*  $t_{\text{arrival}}$  ( $y = 135.45x + 42.94$ ; R-sq (adj) = 1.47;  $P = 0.02$ ). Current speed explained 1.8%  
388 of the *Gymnothorax. spp.*  $t_{\text{maxN}}$  ( $y = 315.57x + 191.45$ ; R-sq (adj) = 1.8;  $P = 0.018$ ) and population  
389 abundance had a significant impact on *E. fasciatus*  $t_{\text{maxN}}$  ( $y = 1792.8x + 6614.5$ ; R-sq (adj) = 6.71%;  $P <$   
390 0.0001). Staying time had no effect upon indices for both tropical models.

391

392 Only population abundance input into models of the Antarctic asteroid *O. validus* movement around the  
393 BUC explained a significant proportion of the  $\text{Max}_N$  values generated ( $y = 0.53x - 0.92$ ; R-sq (adj) = 49.32;  
394  $P < 0.0001$ ). *O. validus*  $t_{\text{arrival}}$  and  $t_{\text{MaxN}}$  values were also only significantly affected by input abundance ( $y =$   
395  $-234.17x + 5199.6$  and  $y = -23.84 + 4915.4$ ; R-sq (adj) = 19.14 and 3.37;  $P < 0.0001$  and  $P = 0.0008$ ). For  
396 *P. corrugatus* input abundance accounted for 34.48% of the variability in  $\text{Max}_N$  ( $y = 0.2241 - 0.0985$ ; R-sq  
397 (adj) = 34.4;  $P < 0.0001$ ) and  $t_{\text{arrival}}$  and  $t_{\text{maxN}}$  19.29% and 1.49% ( $y = -163.74 + 4879.5$  and  $y = -15.179 +$   
398  $4662.0$ ; R-sq (adj) = 19.29 and 1.49;  $P < 0.0001$  and  $P = 0.03$ ). Current speed and *P. corrugatus* approach  
399 speed had no significant effect upon  $\text{Max}_N$ ,  $t_{\text{arrival}}$  and  $t_{\text{maxN}}$  values.

400

### 401 3.2. Comparison to baited underwater camera data

402

403 The  $\text{Max}_N$  output of the models developed to describe the behaviour of the two tropical fish and  
404 Antarctic invertebrate species were all primarily affected by the input parameter population abundance.  
405 Therefore,  $\text{Max}_N$  was only used to match arrival patterns from the in-situ BUC deployment and the multiple  
406 model arrival patterns.  $T_{\text{arrival}}$  and  $t_{\text{maxN}}$  were also significantly related to abundance and could also be  
407 potentially used to select model arrival patterns. There was limited evidence from the sensitivity analysis of  
408 the effect of the other model parameters on the model abundance indices therefore parameters were kept  
409 within the ranges reported in Table 1.

410

411 For 10 of the BUC deployments the corresponding UVC recorded no groupers and for three of the UVC  
412 transects that observed groupers none were observed in corresponding BUC deployments. 10  
413 corresponding UVC and BUC pairs both recorded *E. fasciatus* and for 9 of these pairs the BUC model  
414 produced the same or slightly higher abundance estimates (Fig. 3a). The Bland Altman plot provides little  
415 evidence of systematic bias between the abundance estimates of the grouper *E. fasciatus* generated by the  
416 BUC model methodology and the UVC surveys. This is concluded as all data points are within the +/- 1.96  
417 SD limits of agreement in the plots and points are distributed symmetrically around the mean (Fig.4a). Only  
418 4 corresponding UVC and BUC pairs both observed moray eels of the genus *Gymnothorax* and the BUC  
419 model produced higher or the same abundances. Moray eels were only observed in BUCs in 8 of the  
420 corresponding UVC and BUC pairs and only in UVC in 4 pairs. The Bland-Altman plot show that points  
421 are symmetrically distributed around the mean and that all point were within the +/- 1.96 SD limits of  
422 agreement (Fig.4b).

423

424 In all 18 UVC and BUC pairs *O. validus* was observed and there was no clear pattern of differences  
425 between the abundance estimates recorded by each method (Fig.3c). All the data points for *O. validus*  
426 abundance estimates from the BUC model and the UVC were within or on the +/- 1.96 SD limits of

427 agreement. From the plot it would however, appear that the plots were slightly asymmetrical to the zero and  
428 that average abundances from the model are slightly less than those recorded by the UVC as the abundance  
429 of *O. validus* increases (Fig.4c). For 8 of the 18 corresponding transect and BUC model pairs abundance  
430 estimates for *P. corrugatus* were only recorded by the BUC model and in a further 6 pairs the BUC model  
431 estimates were much larger than in the UVC surveys (Fig.3d). In the Bland-Altman plots two outliers were  
432 removed where abundances > 100 individuals were recorded by the BUC. All points were within the 1.96  
433 SD limits of agreement but they were not symmetrically distributed around the mean indicating that higher  
434 abundances were measured by the BUC (Fig.4d).

435

#### 436 **4. Discussion**

437

438 Results from the sensitivity analysis indicate that for tropical and Antarctic models of fish and  
439 invertebrate movement around the BUC system the abundance of the surveyed population was the factor  
440 most strongly related to the Max<sub>N</sub>. These models allow a BUC user to determine the relationship between  
441 Max<sub>N</sub> and the abundance of the focal species and allow the commonly collected Max<sub>N</sub> unit of relative  
442 abundance to be converted to absolute units. Two other commonly-recorded indices of abundance, t<sub>arrival</sub>  
443 and t<sub>maxN</sub> appear to be less closely related to absolute abundance than might have been assumed, but might  
444 usefully contribute to model parameter selection where more than one abundance value results in the  
445 observed Max<sub>N</sub>. Within the range of species used here, estimates of their searching speed and staying time  
446 had relatively little influence on the model Max<sub>N</sub>. This is a reassuring finding as it is relatively difficult to  
447 estimate these behavioural values in wild animals.

448

449 For all species-specific, models Max<sub>N</sub> appeared to be the measure which accounted for most of the  
450 variability in the input population abundance fish or invertebrates. Measurements of t<sub>arrival</sub> and t<sub>maxN</sub> would  
451 however, reflect more about aspects of fish approach swimming speed and the current velocity observed  
452 around the BUC deployment. Stoner et al., (2008) found that a poor correlation exists between BUC time  
453 based metrics and abundance estimates of juvenile Pacific cod from corresponding seine net trawls, while  
454 Max<sub>N</sub> measures correlated well with trawl survey results. Time based metrics from BUC studies in the  
455 abyssal environment have however, been used successfully to calculate the absolute abundance of  
456 scavenging fish populations (Priede and Merrett, 1996). The current speeds observed around the BUC  
457 deployments and that were used for model ranges were relatively slow. If BUC deployments were within  
458 environments experiencing high current speeds then possibly variation in current speed would likely have a  
459 greater affect on BUC output indices and detailed current speed measurements during BUC deployments  
460 would be essential. The model framework presented here allows these different scenarios to be tested  
461 against field data. Estimates of the range of diffusional velocities experienced in the tropical and Antarctic  
462 environments were not available to investigate its potential effect upon arrival patterns, but again the  
463 framework allows easy incorporation of new field or laboratory data on diffusion to be incorporated as it  
464 becomes available. The incorporation of fluid dynamics modelling into the methodology would enable the  
465 potential effects of current speed and diffusional velocity on the arrival of fish or invertebrates at the BUC  
466 to be explored in more detail. Unlike previous models an odour plume of any shape or concentration can be

467 incorporated into this framework to replace the “pie segment” used here. Animals contacted by the plume or  
468 walking/swimming into the side of it would respond in the same way as those in the existing models.  
469 Refinements such as animals resuming random movement if they leave an irregularly shaped plume would  
470 be added at this stage.

471

472 Staying time had no impact on abundance metrics even though it had been shown to affect  $Max_N$  values  
473 in the deep-sea BUC studies (Priede et al., 1990). The majority of BUC studies in the abyssal northeast  
474 Atlantic found the mean staying time of the deep-sea grenadier (*C. armatus*) to be approximately 2 hours  
475 (Priede et al., 1994; Henriques et al., 2002). In the shallow water BUC fish arrive more rapidly and  
476 frequently, causing the staying time to likely have less of an impact on  $Max_N$  values. With longer staying  
477 times the number of fish at the camera will accumulate to reach  $Max_N$  and the total meaning that  $Max_N$  will  
478 have more of a linear relationship with the numbers visiting the BUC. However, in the shallow water  
479 environment where more fish are coming and going from the field of view there maybe a larger difference  
480 between  $Max_N$  and the total number of animals visiting the camera. These results therefore indicate that in  
481 these models accurate estimate of fish or invertebrate staying time, cruising speed or diffusional velocity are  
482 not important to the output of the model and therefore all that is necessary is the selection of a suitable  
483 range. More important factors such as fish and invertebrate approach speed and the current speed should be  
484 prioritised. The latter is certainly directly measurable at the camera, though in complex habitats the current  
485 experienced by the fauna might be quite different. Approach speed is harder to ascertain, though stereo  
486 camera systems such as BRUVS can probably provide useful information if the system lands facing  
487 downstream at the point at which animals arrive. With downward-looking cameras the field of view is often  
488 too small to get good estimates of movement speed, but not impossible, especially for slow-moving species.  
489 In our Antarctic studies we were able to directly measure invertebrate walking speed across the seabed.

490

491 The absolute abundance estimates of *E. fasciatus* and *O. validus* generated by the BUC model  
492 methodology were found to be most comparable to the abundance estimates from corresponding UVC  
493 surveys. This is because these species are visible to the UVCs as well as to the BUC. The other two species  
494 tend to be hidden in rocks (Clarke and Prothero-Thomas, 1997) or within the coral reef (Bshary et al., 2006)  
495 except when bait is present, with their occasional appearance in the open probably being caused by recent  
496 feeding or disturbance. Moray eels of the genus *Gymnothorax* are generally nocturnal hunters and during  
497 the day they will remain hidden within rocky refuge (Bshary et al., 2006; Bardach et al., 1959) making it  
498 difficult for daytime UVC surveys to detect them. In a number of BUC and UVC corresponding pairs the  
499 BUC survey observed moray eels when the UVC surveys recorded none causing the BUC model to estimate  
500 abundances when the UVC estimate equalled zero. The abundance estimates generated by the BUC models  
501 for the nemertean worm *P. corrugatus* were higher than those within the higher abundance estimates were  
502 produced by the BUC models for *P. corrugatus* due to the BUC recording *P. corrugatus* but none being  
503 observed in the corresponding UVC survey. This can be attributed to the species taking refuge under rocks  
504 during the day (Clarke et al., 1997) causing few to be observed in daytime transects. This will result in the  
505 model parameters being calibrated to artificially low populations densities. Little is known about the  
506 behaviour of *P. corrugatus* and it is possible that large groups of individuals congregate within refuges

507 (Clarke and Prothero-Thomas, 1997), violating the assumption of the model that individuals are randomly  
508 distributed and act independently of each other.

509

510 Models also assume that all fish react and follow the bait plume once encountered, however factors such  
511 as satiation state, olfactory capabilities and the availability of other food sources in the environment will  
512 impact upon their decision. Due to the comparability of absolute abundance estimates from the BUC model  
513 and the UVC, it would appear that a large proportion of the nearby animals from these species reacted to the  
514 bait plume. Model assumptions include that individuals react independently of each other however,  
515 competitive behavioural interactions have been observed to occur between fish at the bait of BUC systems  
516 (Armstrong et al., 1992; Stoner et al., 2008; Dunlop et al., 2014). It has been suggested that these  
517 interactions discourage some fish from approaching the bait due to the increased chance of competition  
518 (Jones et al., 2013; Willis et al., 2003; Cappo et al., 2004) or predation (Lampitt et al., 1983; Harvey et al.,  
519 2007) presented by the other fish. It is therefore evident that in both the fish species studied competitive  
520 interactions around the BUC could potentially impact upon the arrival patterns of individuals at the bait.  
521 The effect of other species interactions on the arrival patterns of fish and invertebrates at the BUC should  
522 also be considered. Effects may include particular species posing a higher predation risk at the bait  
523 reducing the number of the other species observed. Further studies of the impact of these interactions would  
524 allow this information to be added to modelling approaches. Unlike previous models our framework would  
525 allow multiple species models to be combined using information on the species composition and potentially  
526 the effects of interactions on bait approach and staying times. Also when foraging individuals become close  
527 to the bait they are potentially attracted by the movement and sounds of others feeding (Bailey and Priede,  
528 2002). For shallow water fish species that rely heavily upon sight for foraging and hunting (Stoner et al.,  
529 2008) this has the potential to impact on their behaviour in relation to the BUC system and thus arrival  
530 patterns. Further valuable research would be the investigation of the application of this modelling approach  
531 to other marine species, which have been found to be attracted to BUC systems. This would primarily  
532 include the large, predatory mobile species that BUC surveys have been found to effectively survey  
533 (Malcolm et al., 2007; Watson et al., 2010).

534

535 Preliminary results show that this stochastic modelling approach can generate absolute abundance  
536 estimates of some shallow water fish and invertebrate populations from BUC deployments and that these  
537 estimates are comparable to an established survey method. Discrepancies were apparently due to cryptic  
538 behaviour in some species resulting in underestimates of abundance during underwater visual census  
539 surveys. The generation of absolute abundance estimates from shallow BUC surveys improves the  
540 application of the method substantially and makes the results comparable to those of other survey methods,  
541 such as trawl surveys and transects commonly used in stock assessments and monitoring programmes. This  
542 also enables previously-collected BUC data to be reanalysed and diversity indices for these deployments to  
543 be recalculated based on the abundances of the animals present rather than combinations of  $Max_N$  values.

544

545 In conclusion, the spatial, stochastic modelling approach described and tested in this study represents  
546 one of the first attempts to model the arrival process of shallow water marine species at a BUC system.

547 Initial results for a small set of tropical and Antarctic species-specific models show that this method has the  
548 potential to generate absolute abundance estimates from BUC data that are comparable to UVC data. The  
549 model could be used retrospectively to re-analyse existing Max<sub>N</sub> data. This development combined with the  
550 existing ability of BUCs to generate data in a time-and-cost efficient and non-destructive manner can  
551 significantly improve the value of this method to monitor inshore marine populations.

552

553

## 554 **Figure and Table Legends**

555

556 **Fig. 1.** Diagram illustrating the general input and output parameters of the model simulation describing the  
557 behaviour of fish and invertebrate populations in relation to a baited underwater camera system.

558

559 **Fig. 2.** Example plot of the arrival pattern of the black tip grouper (*Epinephelus fasciatus*) at the baited  
560 underwater camera system (BUC) produced by 5 model runs and the arrival pattern from an in-situ BUC  
561 deployment.

562

563 **Fig. 3.** Histograms and scatter plots comparing the absolute abundance estimates generate from UVC transects  
564 (open bars) and BUC models (closed bars) for a) the grouper (*Epinephelus fasciatus*), b) the moray eel species  
565 (*Gymnothorax* spp.), c) the Antarctic asteroid (*Odontaster validus*) and d) the Antarctic nemertean worm  
566 (*Parbolasia corrugatus*).

567

568 **Fig. 4.** Bland Altman plots illustrating the agreement between the abundance estimates generated by the  
569 baited underwater camera model (BUC) and the underwater visual census survey (UVC) for a) *Epinephelus*  
570 *fasciatus*, b) *Gymnothorax* spp., c) *Odontaster validus* and d) *Parbolasia corrugatus*.

571

572 **Table 1** Input parameters ranges for *Epinephelus fasciatus*, *Gymnothorax* spp., *Pollachius virens*,  
573 *Scyliorhinus canicula*, *Odontaster validus* and *Parbolasia corrugatus*.

574

## 575 **Acknowledgements**

576

577 This research was supported by a University of Glasgow Faculty Scholarship to KMD, a Collaborative  
578 Gearing Scheme grant from the Natural Environmental Research Council and the British Antarctic Survey  
579 and an ASSEMBLE infrastructure access grant to DMB. The authors would like to thank the staff of the  
580 Inter-University Institute of Marine Sciences (IUI), Eilat, in particular Asaph Rivlin, Oded Ben-Shaprut and  
581 Simon Berkowitz, and the diving and boating teams at Rothera Research Station, Western Antarctic  
582 Peninsula, in particular Dr David Barnes and Ashley Cordingley. Permits were received from the Israel  
583 Nature and Parks Agency and the authors thank both organisations for allowing us to conduct this work.

584 **References**

585

586 Armstrong, J.D., Bagley, P.M., Priede, I.G., 1992. Photographic and acoustic tracking observations of the  
587 behaviours of the grenadier *Coryphaenoides (Nematoburus) armatus*, the eel *Synaphobranchus bathybius*,  
588 and other abyssal demersal fish in the North Atlantic Ocean. Mar. Biol. 112, 535-544.

589 Bailey, D.M., Priede, I.G., 2002. Predicting fish behaviour in response to abyssal food falls. Mar. Biol. 141, 831-  
590 840.

591 Bailey, D.M., Wagner, H.J., Jamieson, A.J., Ross, M.F., Priede, I.G., 2007. A taste of the deep-sea: The roles of  
592 gustatory and tactile searching behaviour in the grenadier fish *Coryphaenoides armatus*. Deep. Sea. Res.  
593 54, 99-108.

594 Bardach, J.E., Winn, H.E., Menzel, D.W., 1959. The role of the senses in the feeding of the nocturnal reef predators  
595 *Gymnothorax moringa* and *G. vicinus*. Copeia 1959, 133-139.

596 Bassett, D.K., Montgomery, J.C., 2011. Investigating nocturnal fish populations *in situ* using baited underwater  
597 video: With special reference to their olfactory capabilities. J. Exp. Mar. Biol. Ecol. 409, 194-199.

598 Bland, J.M., Altman, D.G., 1986. Statistical methods for assessing agreement between two methods of clinical  
599 measurement. The Lancet 327, 307-310.

600 Bland, J.M., Altman, D.G., 1995. Comparing methods of measurement: why plotting difference against standard  
601 method is misleading. The Lancet 346, 1085-1087.

602 Brown, T.N., Kulasiri, D., 1996. Validating models of complex, stochastic, biological systems. Ecol. Model. 86,  
603 129-134.

604 Bshary, R., Hohner, A., Ait-el-Djoudi, K., Fricke, H., 2006. Interspecific communicative and coordinated hunting  
605 between groupers and giant moray eels in the Red Sea. Plos. Biol. 4, e431.

606 Cappel, M., Speare, P., De'ath, G., 2004. Comparison of baited remote underwater video stations (BRUVS) and  
607 prawn (shrimp) trawls for assessments of fish biodiversity in inter-reefal areas of the Great Barrier Reef  
608 Marine Park. J. Exp. Mar. Biol. 302, 123-152.

609 Charnov, E.L., 1976. Optimal foraging, the marginal value theorem. Theor. Popul. Biol. 9, 129-136.

610 Clarke, A., Prothero-Thomas, E., 1997. The influence of feeding on oxygen consumption and nitrogen excretion in  
611 the Antarctic nemertean *Parborlasia corrugatus*. Physiol. Biochem. Zool. 70, 639-649.

612 Collins, M. A., Yau, C., Nolan, C. P., Bagley, P. M., Priede, I. G., 1999. Behavioural observations on the scavenging  
613 fauna of the Patagonian slope. J. Mar. Biol. Assoc. UK. 79, 963-970.

614 Collins, M.A., Yau, C., Guilfoyle, F., Bagley, P., Everson, I., Priede, I., Agnew, D., 2002. Assessment of stone crab  
615 (Lithodidae) density on the South Georgia slope using baited video cameras. Ices. J. Mar. Sci. 59, 370-379.

616 D'Aout, K., Aerts, P., 1999. A kinematic comparison of forward and backward swimming in the eel *Anguilla*  
617 *anguilla*. J. Exp. Biol. 202, 1511-1521.

618 Dorman, S.R., Harvey, E.S., Newman, S.J., 2012. Bait effects in sampling coral reef fish assemblages with stereo-  
619 BRUVs. Plos One 7, e41538.

620 Dunlop, K.M., Scott, E.M., Parsons, D., Bailey, D.M., 2014. Do agonistic behaviours bias baited remote underwater  
621 video surveys of fish? Mar. Ecol. (in press).

622 Ellis, D., DeMartini, E., 1995. Evaluation of a video camera technique for indexing abundances of juvenile pink  
623 snapper, *Pristipomoides filamentosus*, and other Hawaiian insular shelf fishes. Fishery B-NOAA 93, 67-77

624 Farnsworth, K.D., Thygesen, U.H., Ditlevsen, S., King, N.J., 2007. How to estimate scavenger fish abundance using  
625 baited camera data. Mar. Ecol. Prog. Ser. 350, 223-234.



- 626 Fitzpatrick, B.M., Harvey, E.S., Heyward, A.J., Twiggs, E.J., Colquhoun, J., 2012. Habitat specialization in tropical  
627 continental shelf demersal fish assemblages. *Plos One* 7, e39634.
- 628 Fulton, C.J., 2007. Swimming speed performance in coral reef fishes: field validations reveal distinct functional  
629 groups. *Coral Reefs* 26, 217-228.
- 630 Gibran, F. Z., 2007. Activity, habitat use, feeding behavior, and diet of four sympatric species of Serranidae  
631 (Actinopterygii: Perciformes) in southeastern Brazil. *Neotrop. Ichthyol.* 5, 387-398.
- 632 Harvey, E.S., Cappo, M., Butler, J.J., Hall, N., Kendrick, G.A., 2007. Bait attraction affects the performance of  
633 remote underwater video stations in assessment of demersal fish community structure. *Mar. Ecol. Prog. Ser.*  
634 350, 245-254.
- 635 Harvey, E.S., Newman, S.J., McLean, D.L., Cappo, M., Meeuwige, J.J., Skepperb, C.L., 2012. Comparison of the  
636 relative efficiencies of stereo-BRUVs and traps for sampling tropical continental shelf demersal fishes.  
637 *Fish. Res.* 125, 108-120.
- 638 Heagney, E.C., Lynch, T.P., Babcock, R.C., Suthers, I.M., 2007. Pelagic fish assemblages assessed using mid-water  
639 baited video: Standardising fish counts using bait plume size. *Mar. Ecol. Prog. Ser.* 350, 255-266.
- 640 Henriques, C., Priede, I.G., Bagley, P.M., 2002. Baited camera observations of deep-sea demersal fishes of the  
641 northeast Atlantic Ocean at 15-28 degrees N off West Africa. *Mar. Biol.* 141, 307-314.
- 642 Johnson, A.F., Jenkins, S.R., Hiddink, J.G., Hinz, H., 2012. Linking temperate demersal fish species to habitat:  
643 scales, patterns and future directions. *Fish. Fish.* 14, 256-280.
- 644 Jones, E.G., Tselepidis, A., Bagley, P.M., Collins, M.A., Priede, I.G., 2003. Bathymetric distribution of some  
645 benthic and benthopelagic species attracted to baited cameras and traps in the deep eastern Mediterranean.  
646 *Mar. Ecol. Prog. Ser.* 251, 75-86.
- 647 Kidawa, A., 2001. Antarctic starfish, *Odontaster validus*, distinguish between fed and starved conspecifics. *Polar.*  
648 *Biol.* 24, 408-410.
- 649 King, N.J., Bagley, P.M., Priede, I.G., 2006. Depth zonation and latitudinal distribution of deep-sea scavenging  
650 demersal fishes of the Mid-Atlantic Ridge, 42 to 53 degrees N. *Mar. Ecol. Prog. Ser.* 319, 263-274.
- 651 King, N.J., Jamieson, A.J., Bagley, P.M., Priede, I.G., 2008. Deep-sea scavenging demersal fish fauna of the Nazare  
652 Canyon system, Iberian coast, north-east Atlantic Ocean. *J. Fish. Biol.* 72, 1804-1814.
- 653 Lampitt, R.S., Merrett, N.R., Thurston, M.H., 1983. Interrelations of necrophagous amphipods, a fish predator, and  
654 tidal currents in the deep-sea. *Mar. Biol.* 74, 73-78.
- 655 Langlois, T.J., 2006. Baited underwater video for assessing reef fish populations in marine reserves. *SPC Newsletter*  
656 118, 53-57.
- 657 Langlois, T.J., Fitzpatrick, B.R., Fairclough, D.V., Wakefield, C.B., Hesp, S.A., McLean, D.L., Harvey, E.S.,  
658 Meeuwig, J.J., 2012. Similarities between line fishing and baited stereo-video estimations of length-  
659 frequency: Novel application of kernel density estimates. *Plos One* 7, e45973-e45973.
- 660 Langlois, T.J., Harvey, E.S., Fitzpatrick, B., Meeuwig, J.J., Shedrawi, G., Watson, D.L., 2010. Cost-efficient  
661 sampling of fish assemblages: comparison of baited video stations and diver video transects. *Aquat. Biol.* 9,  
662 155-168.
- 663 Malcolm, H.A., Gladstone, W., Lindfield, S., Wraith, J., Lynch, T.P., 2007. Spatial and temporal variation in reef  
664 fish assemblages of marine parks in New South Wales, Australia - baited video observations. *Mar. Ecol.*  
665 *Prog. Ser.* 350, 277-290.
- 666 McLean, D.L., Harvey, E.S., Fairclough, D.V., Newman, S.J., 2010. Large decline in the abundance of a targeted  
667 tropical lethrinid in areas open and closed to fishing. *Mar. Ecol. Prog. Ser.* 418, 189-199.

- 668 Meager, J.J., Batty, R.S., 2007. Effects of turbidity on the spontaneous and prey-searching activity of juvenile  
669 Atlantic cod (*Gadus morhua*). Philos. Trans. R. Soc. Lond. B. Biol. Sci. 362, 2123-2130.
- 670 Moore, C.H., Harvey, E.S., Van Niel, K., 2010. The application of predicted habitat models to investigate the spatial  
671 ecology of demersal fish assemblages. Mar. Biol. 157, 2717-2729.
- 672 Priede, I.G., Bagley, P.M., 2000. In situ studies on deep-sea demersal fishes using autonomous unmanned lander  
673 platforms. Oceanog. Mar. Biol. 38, 357-392.
- 674 Priede, I.G., Bagley, P.M., Smith, A., Creasey, S., Merrett, N.R., 1994. Scavenging deep demersal fishes of the  
675 Porcupine Seabright, Northeast Atlantic - Observations by baited camera, trap and trawl. J. Mar. Biol.  
676 Assoc. UK. 74, 481-498.
- 677 Priede, I.G., Merrett, N.R., 1996. Estimation of abundance of abyssal demersal fishes; A comparison of data from  
678 trawls and baited cameras. J. Fish. Biol. 49, 207-216.
- 679 Priede, I.G., Smith, K.L., Armstrong, J.D., 1990. Foraging behaviour of abyssal grenadier fish. Inferences from  
680 acoustic tagging and tracking in the North Pacific Ocean. Deep. Sea. Res. 37, 81-101.
- 681 Reidenbach, M.A., Koehl, M., 2011. The spatial and temporal patterns of odors sampled by lobsters and crabs in a  
682 turbulent plume. J. Exp. Biol. 214, 3138-3153.
- 683 Sainte-Marie, B., Hargrave, B.T., 1987. Estimation of scavenger abundance and distance of attraction to bait. Mar.  
684 Biol. 94, 431-443.
- 685 Saltelli, A., Chan, K., Scott, E.M., 2000. Sensitivity analysis. New York, Wiley.
- 686 Sigler, M.F., 2000. Abundance estimation and capture of sablefish (*Anoplopoma fimbria*) by longline gear. Can J  
687 Fish. Aquat. Sci. 57, 1270-1283.
- 688 Smale, D.A., Barnes, D.K.A., Fraser, K.P.P., Mann, P.J., Brown, M.P., 2007. Scavenging in Antarctica: Intense  
689 variation between sites and seasons in shallow benthic necrophagy. J. Exp. Mar. Biol. Ecol. 349, 405-417.
- 690 Stobart, B., Garcia-Charton, J.A., Espejo, C., Rochel, E., Goni, R., Renones, O., Herrero, A., Crec'hriou, R., Polti,  
691 S., Marcos, C., Planes, S., Perez-Ruzafa, A., 2007. A baited underwater video technique to assess shallow-  
692 water Mediterranean fish assemblages: Methodological evaluation. J. Exp. Mar. Biol. Ecol. 345, 158-174.
- 693 Stoner, A., 2004. Effects of environmental variables on fish feeding ecology: implications for the performance of  
694 baited fishing gear and stock assessment. J. Fish. Biol. 65, 1445-1471.
- 695 Stoner, A.W., Ryer, C.H., Parker, S.J., Auster, P.J., Wakefield, W.W., 2008. Evaluating the role of fish behavior in  
696 surveys conducted with underwater vehicles. Can. J. Fish. Aquat. Sci. 65, 1230-1243.
- 697 Taylor, M.D., Baker, J., Suthers I.M., 2013. Tidal currents, sampling effort and baited remote underwater video  
698 (BRUV) surveys: Are we drawing the right conclusions? Fish. Res. 140, 96-104.
- 699 Watson, D.L., Anderson, M.J., Kendrick, G.A., Nardi, K., Harvey, E.S., 2009. Effects of protection from fishing on  
700 the lengths of targeted and non-targeted fish species at the Houtman Abrolhos Islands, Western Australia.  
701 Mar. Ecol. Prog. Ser. 384, 241-249.
- 702 Watson, D.L., Harvey, E.S., Fitzpatrick, B.M., Langlois, T.J., Shedrawi, G., 2010. Assessing reef fish assemblage  
703 structure: how do different stereo-video techniques compare? Mar. Biol. 157, 1237-1250.
- 704 Westera, M., Lavery, P., Hyndes, G., 2003. Differences in recreationally targeted fishes between protected and  
705 fished areas of a coral reef marine park. J. Exp. Mar. Biol. Ecol. 294, 145-168.
- 706 Willis, T.J., Babcock, R.C., 2000. A baited underwater video system for the determination of relative density of  
707 carnivorous reef fish. Mar. Freshwater. Res. 51, 755-763.

708 Willis, T.J., Millar, R.B., Babcock, R.C., 2003. Protection of exploited fish in temperate regions: High  
709 density and biomass of snapper *Pagrus auratus* (Sparidae) in northern New Zealand marine  
710 reserves. J. Appl. Ecol. 40, 214-227.



Figure 1

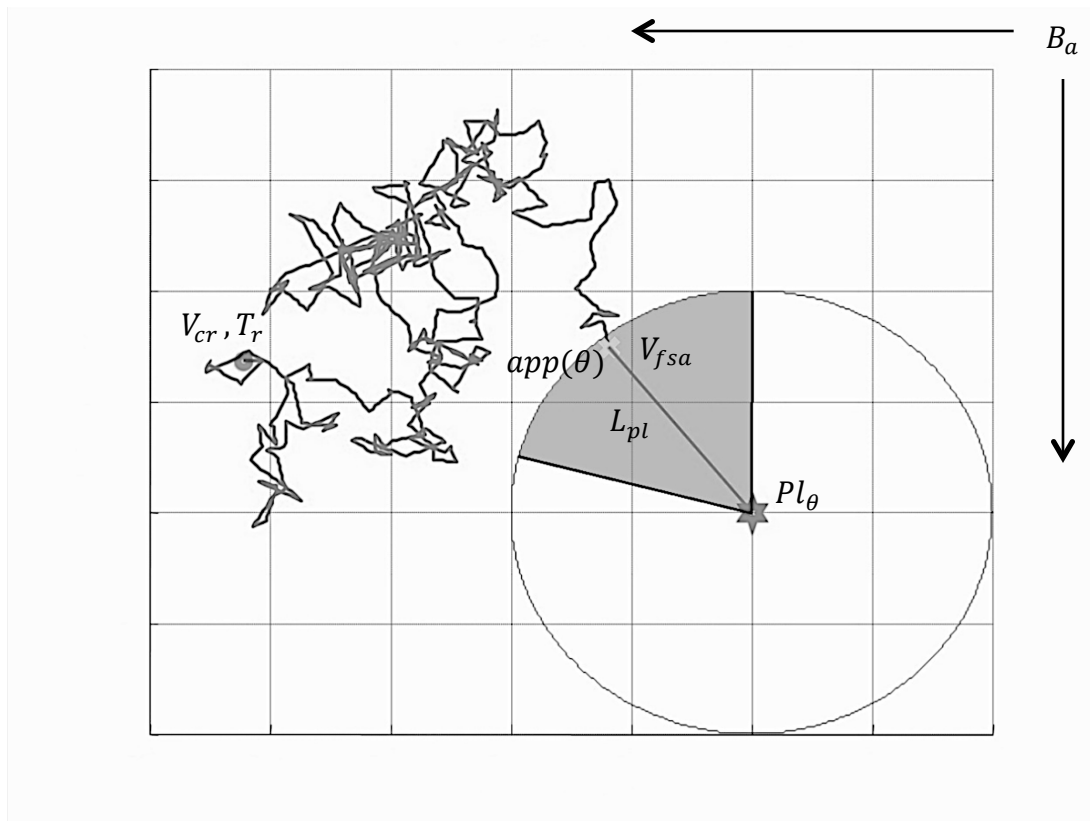


Figure 2

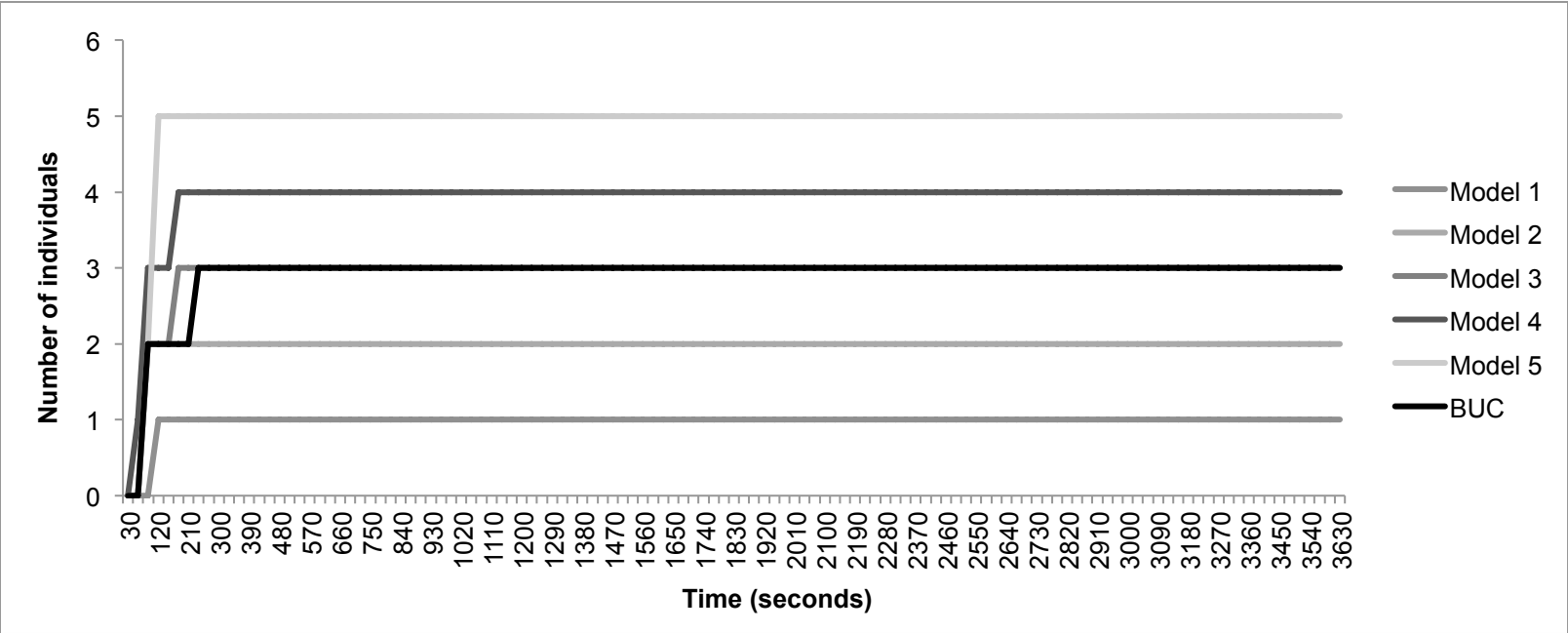
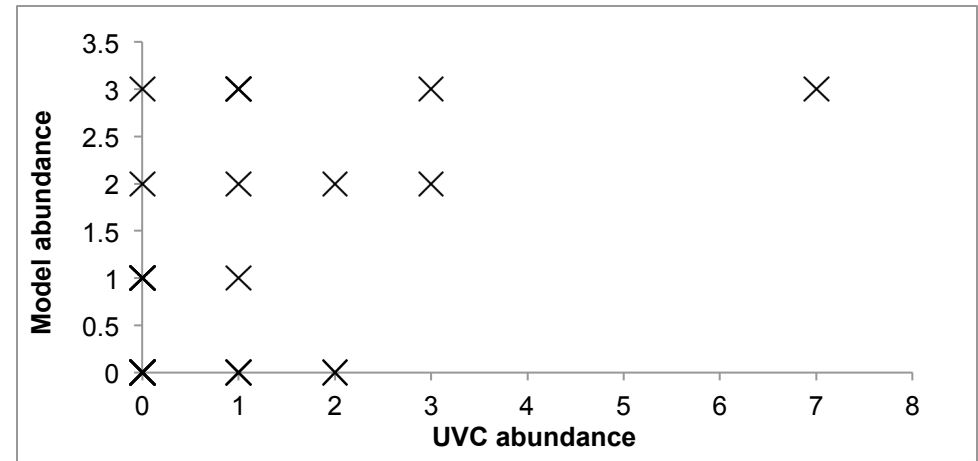
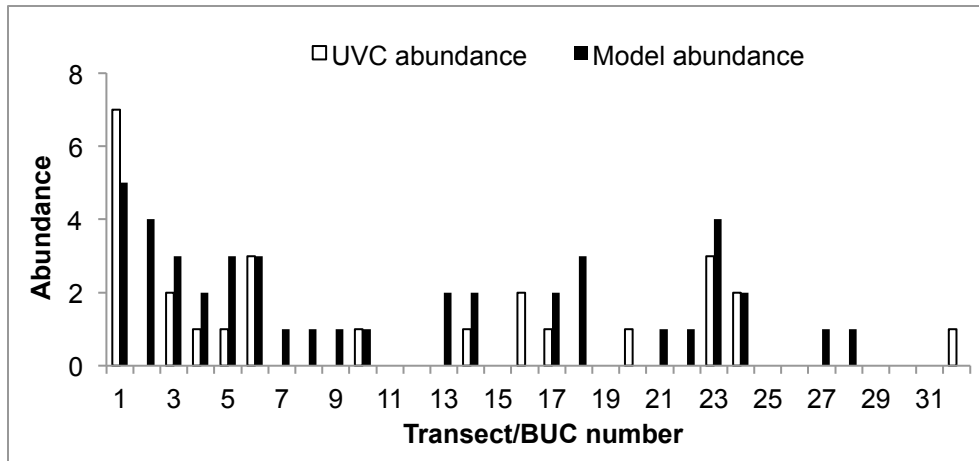
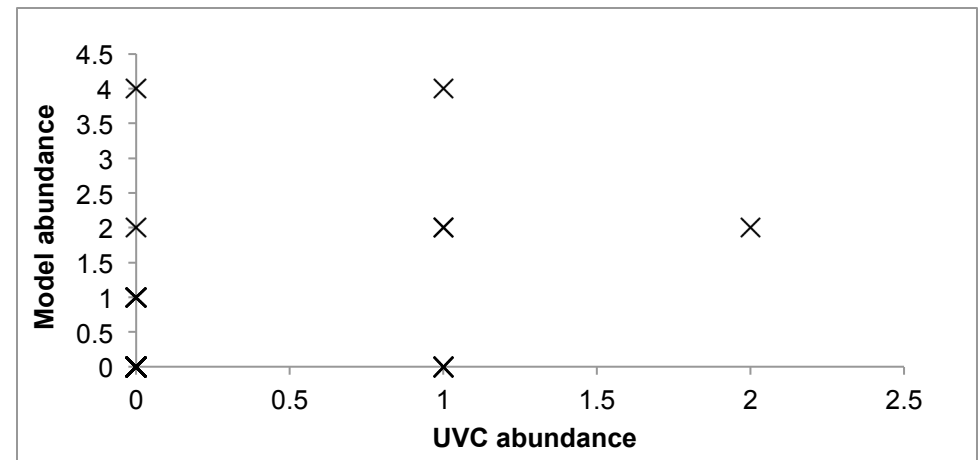
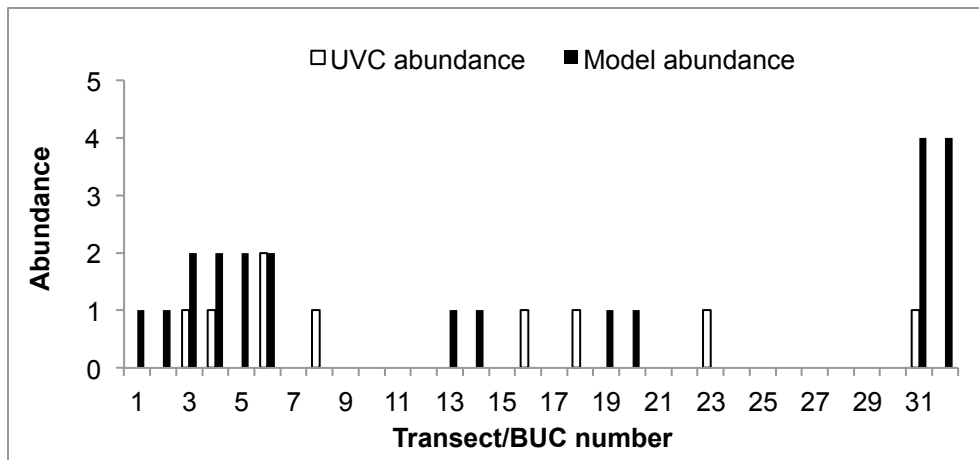


Figure 3

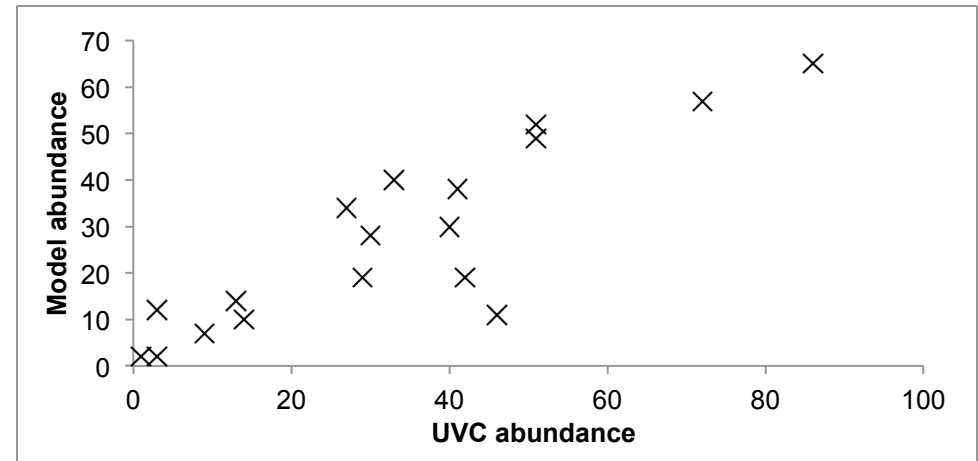
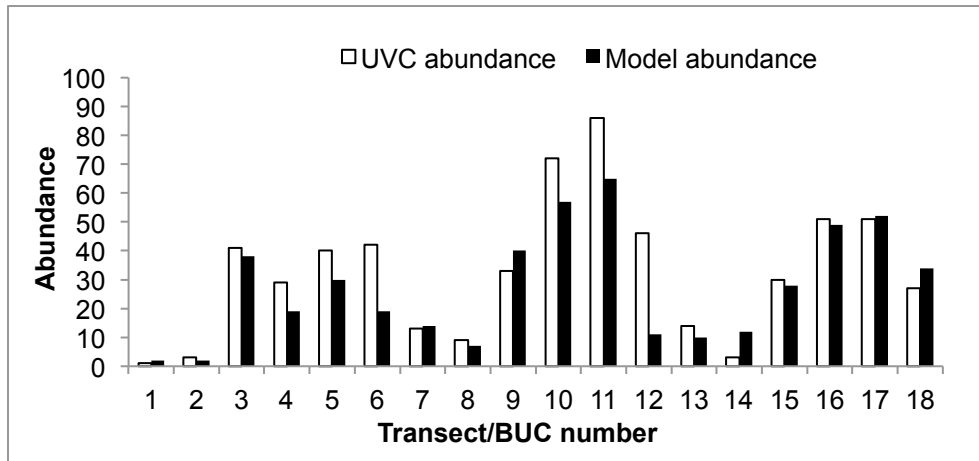
a) *Epinephelus fasciatus*



b) *Gymnothorax* spp.



c) *Odontaster validus*



d) *Parabolasia corrugatus*

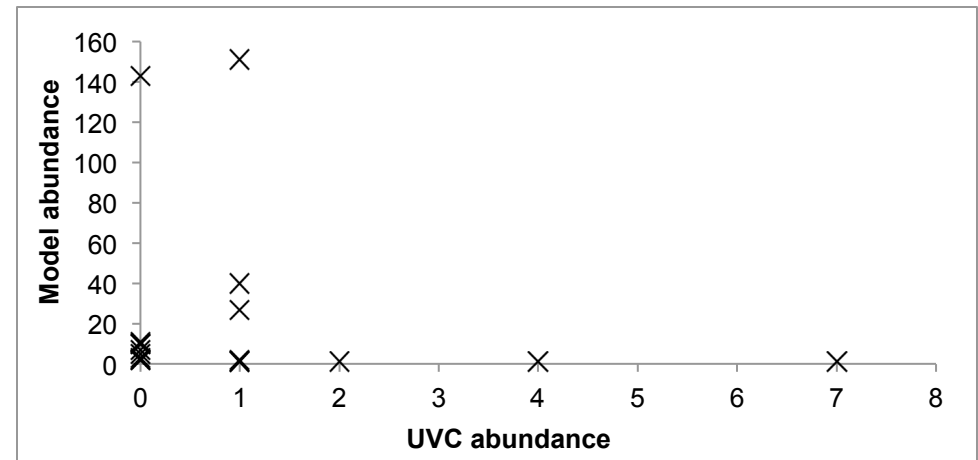
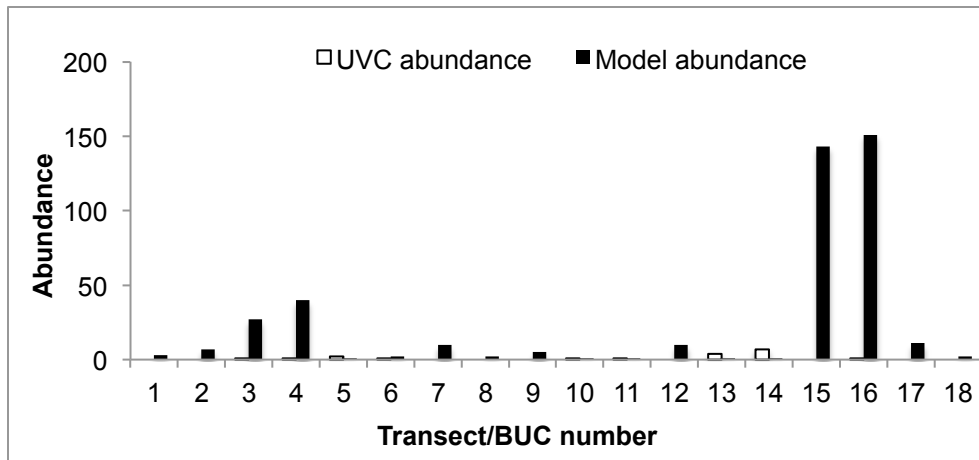
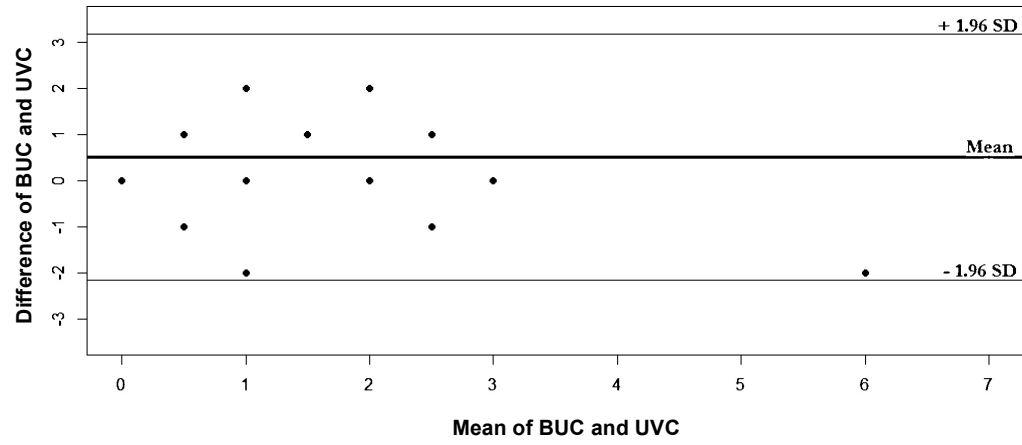




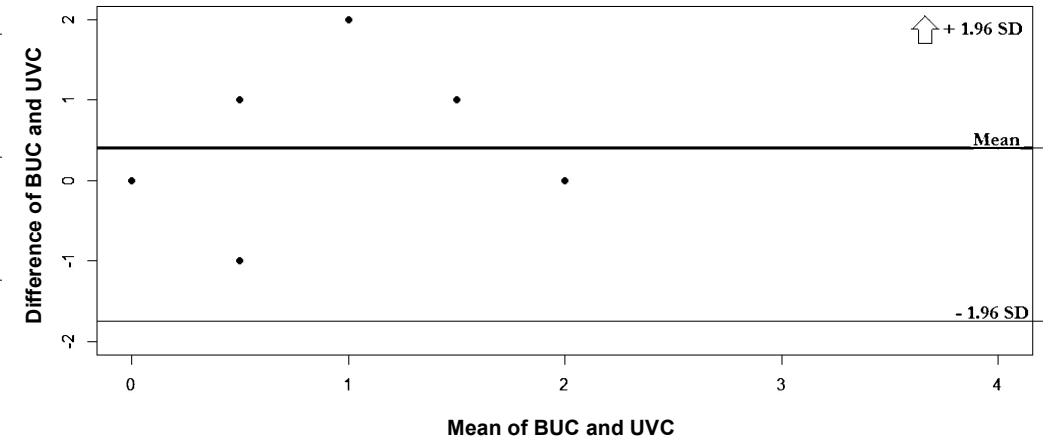


Figure 4

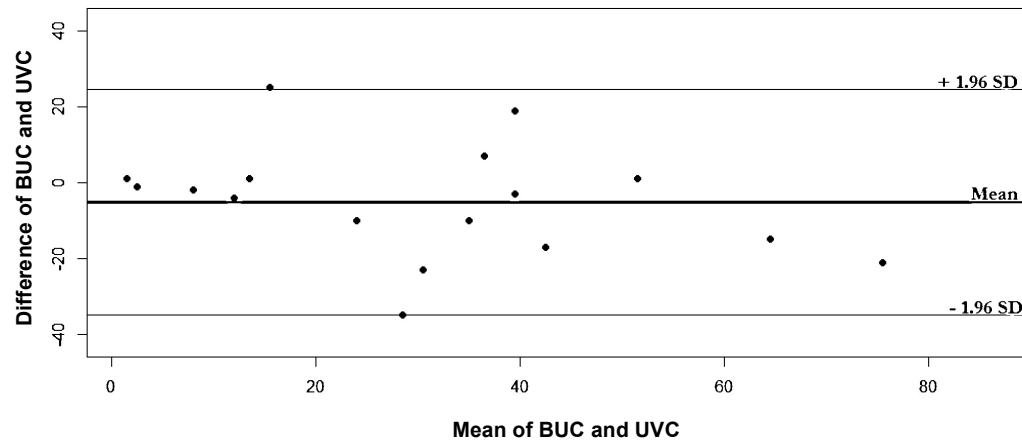
A



B



C



D

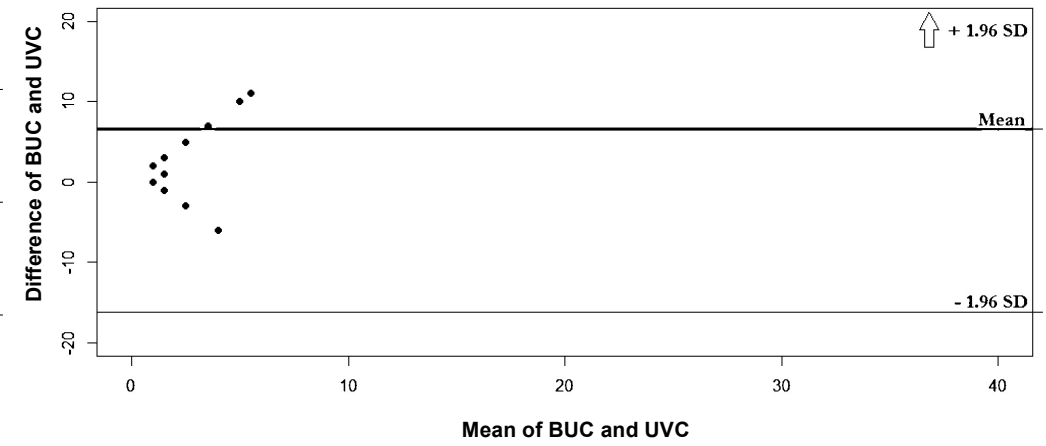


Table 1

Parameters	Area (m <sup>2</sup> )	Current speed (m s <sup>-1</sup> )	Abundance (individuals)	Cruising speed (m s <sup>-1</sup> )	Turning interval (s)	Approach speed (m s <sup>-1</sup> )	Staying time (s)	References
<b>Species</b>								
<i>Epinephelus fasciatus</i>	1000	0.02 - 0.2	1 - 100	0 – 0.2	0 - 120	0.294 - 0.365	0 - 240	Fulton, 2007; Bshary et al., 2006
<i>Gymnothorax</i> spp.	1000	0.02 - 0.2	1 - 100	0	0 - 120	0.0935 - 0.318	0 - 180	D'Aout and Aerts, 1999; Gibran, 2007
<i>Odontaster validus</i>	6.25	0.01 - 0.1	1 - 100	0	n/a	0.0001 – 0.001	To simulation end	Kidawa, 2001
<i>Parbolasia corrugatus</i>	6.25	0.01 – 0.1	1 - 100	0	n/a	0.0001 – 0.0003	To simulation end	Clarke and Prothero-Thomas, 1997

